ISSN: 0975-833X

Available online at http://www.journalcra.com

International Journal of Current Research
Vol. 18, Issue, 01, pp.36077-36085, January, 2026
DOI: https://doi.org/10.24941/ijcr.49932.01.2026

INTERNATIONAL JOURNAL OF CURRENT RESEARCH

RESEARCH ARTICLE

PERFORMANCE EVALUATION OF ACTIVATED CARBON FROM NEEM SEED SHELLS (AZADIRACHTA INDICA A. JUSS) FOR THE REMOVAL OF COMPLEX MIXTURE OF DYE (METHYLENE BLUE) AND HEAVY METALS (COPPER, NICKEL AND IRON)

Adama DIOP[1*], Mamadou FAYE[1,2], Djibril DIEDHIOU[1,2,3], Papa Lat Dior DIOP[1], Mbaye WADE[1] and Codou Guèye Mar DIOP[1]

[1]Université Cheikh Anta DIOP(UCAD), Ecole Supérieure Polytechnique (ESP), Laboratoire Eau, Energie, Environnement et Procédés Industriels (LE3PI), BP5085 Fann-Dakar, Sénégal; [2]Institut National Polytechnique (INP), Ecole Nationale Supérieure des Ingénieurs en Arts Chimiques et Technologiques (ENSIACET), UMR 1010 Laboratoire de Chimie Agro-Industrielle, BP 44362 - 31030 Toulouse Cedex 4, France; [3]Université du Sine Saloum El Hadji Ibrahima Niass (USSEIN), UFR, Sciences Fondamentales et de l'Ingénieur, BP 55 Kaolack, Sénégal

ARTICLE INFO

Article History:
Received 25th October, 2025
Received in revised form
20th November, 2025
Accepted 18th December, 2025
Published online 30th January, 2026

Keywords:
Adsorption, Dye, Heavy Metals, Neem Seed Hulls, Complex Mixure.

Corresponding author: **Adama DIOP**

ABSTRACT

Industrial and urban wastewater contributes significantly to environmental pollution. That is why, it is essential that wastewater be treated before being discharged into the environment. The aim of this study is to evaluate the performance of Activated Carbon (AC) from neem seed shells for the removal of a complex mixture of dye and heavy metals (Methylene Blue (MB), copper, nickel and iron) in aqueous solution. The AC used in this study was produced by chemical activation with phosphoric acid (85%) at an impregnation ratio of 1/3, at 120°C for 6 hours, followed by pyrolysis at 528°C for 1 hour. The AC contains has high porosity, methylene blue (39.21 $mg.g^{-1}$), and iodine (788.20 $mg.g^{-1}$) indices, and a heterogeneous surface rich in functional groups (alcohols, carboxylic acids, esters, aldehydes, ketones, ethers and lactones). The study of adsorption kinetics reveals that the pseudo-second order model best describes the adsorption of all the pollutants studied, except for the copper, which is better described by the pseudo-first order model. Isotherm modelling shows that the adsorption of all pollutants, except for the Ni(II) is best explained by the Langmuir model, while that of Ni(II) ions is best described by the Freundlich model. The results indicate that AC is more effective at removing dye than heavy metals, with an affinity order of BM > Ni(II) > Fe(II) > Cu(II). This study shows that neem seed shells, considered waste, are an excellent precursor to produce commercial AC that can be used to treat wastewater.

Citation: Adama DIOP, Mamadou FAYE, Djibril DIEDHIOU, Papa Lat Dior DIOP, Mbaye WADE and Codou Guèye Mar DIOP. 2026. "Performance evaluation of activated carbon from neem seed shells (Azadirachta indica A. Juss) for the removal of complex mixture of dye (methylene blue) and heavy metals (copper, nickel and iron)". ***International Journal of Current Research, 18, (01), 36077-36085.***

INTRODUCTION

In recent years, human activities, particularly industrial activities, have been generating increasingly large quantities of wastewater (Donkadokula et al., 2020; Lakherwal, 2014). This wastewater is generally full of with various types of pollutants that are often toxic, poorly biodegradable and bioaccumulative, such as heavy metals, dyes, pesticides, pharmaceutical compounds, etc. (Anfar et al., 2020; Ani et al., 2020; Ks & Belagali, 2013; Ouyang et al., 2020). The direct discharge of these industrial effluents into the environment without prior treatment contributes significantly to the pollution of surface water and groundwater (Ahsaine et al., 2018). Due to their toxicity, low biodegradability and bioaccumulative nature, strict discharge standards are often imposed to preserve the living environment, the ecosystem, and the environment. Compliance with these standards has led to the development of effective treatment methods for the removal of these multifaceted pollutants before being discharged into receiving environments. Among these methods, adsorption on activated carbon remains the most effective one for the removal of these types of recalcitrant molecules. The objective of this study is, on the one hand, to develop activated carbon from local biomass, particularly neem seed shells, and, on the other hand, to evaluate the effectiveness of the adsorption process for treating complex mixtures of dyes and heavy metals (methylene blue, copper, nickel, and iron) in aqueous solution in order to propose an effective treatment scheme for these toxic and recalcitrant molecules.

MATERIALS AND METHODS

Raw materials introduction and pre-treatment of raw materials: The neem seeds used in this study have collected in Babol (Kaolack, Senegal). They were first dried and sorted, then shelled to separate the shells from the kernels (Figure 1).

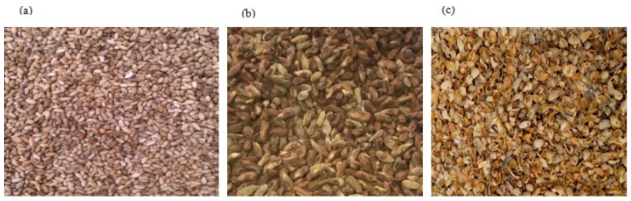

Fig.1.Neem seeds (a), almonds (b) and shells (c)

The shells werethen washed with distilled water, dried at 105°C for 24 hours, werethen crushed and sieved to obtain a powder with a particle size of less than 800 µm, which wasused to prepare the activated carbon.

Activated carbon production process: Activated carbon is prepared by chemical activation with phosphoric acid (H_3PO_4, 85%). Neem shell powder was impregnated with the activation solution at a precursor/activation agent mass ratio of 1:3. The mixture obtained was stirred for 1 hour at room temperature (approximately 25°C) to ensure even distribution of the activation agent (**Figure 2**). After impregnation, the material was dried in an oven at 120°C for 6 hours, then carbonized in a furnace at 528°C for 1 hour. The charcoal obtained was purified by washing with distilled water and dried in an oven at 105°C for 24 hours (**Figure 3**).

Fig.2. Aspect of impregnated shell powders

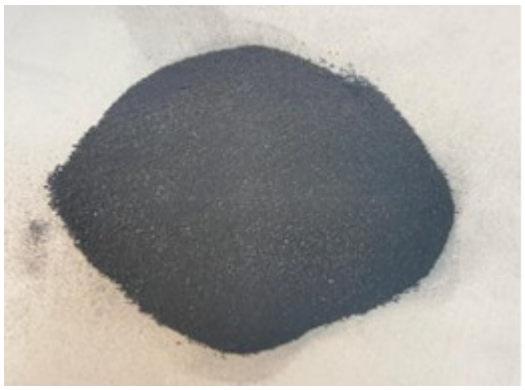

Fig.3. Aspect of activated carbon

Preparation of complex mixtures: The stock solutions of methylene blue and metal salts ($Fe(NH_4)_2(SO_4)_2.6H_2O$, $NiSO_4.6H_2O$ and $CuSO_4$) are prepared by dissolving them in distilled water and then diluted to obtain the desired concentrations.

Characterisation of activated carbon

Determination of pyrolysis yield

The pyrolysis yield reflects the loss of biomass mass. To calculate is we use the following equation:

$$Y = \frac{W_f}{W_i} \times 100$$

Y stands the pyrolysis yield in %; W_f, the weight after pyrolysis in g; W_f, the weight of dry matter before pyrolysis in g.

Determination of moisture content: Moisture content is determined in accordance with standard NF V 03-603 to measure the loss in mass of a sample weighing approximately 1 g that has been dried in an oven at 105°C until a constant mass is obtained.

Determination of ash content: The ash content is determined in accordance with standard NF V 03-922 by incinerating the dry sample at 550°C for 3 hours, then calculated based on the difference in mass before and after incineration.

Determination of volatil materialscontent: The volatile materials content is determined by the loss in mass of a dry sample that was incinerated in an oven at 1000°C for 3 hours.

Determination of pH and electric conductivity: The pH and electrical conductivity are determined in accordance with ASTM 3838-80 method(Elango & Govindasamy, 2018). To do this, approximately 1 g of sample is added to 100 mL of distilled water and stirred continuously at a speed of 1500 rpm for 1 hour at 25°C. The pH and conductivity of the filtrate are then measured using a multifunction pH meter (HI 2211, Hanna Instruments, French)

Determination of bulk density: The apparent density is determined by using a graduated test tube by relating the mass of the adsorbent to the apparent volume occupied using the following formula:

$$BD = \frac{W}{V}$$

BD is the bulk density of the sample in $g.cm^{-3}$; W is the weight of the sample in g and V is the volume occupied by the sample in cm^{-3}.

Determination of true density: The true density is determined using a graduated cylinder by relating the mass of the adsorbent to the apparent volume occupied using the following formula:

$$TD = \frac{W}{V}$$

With:

$$V = V_{ep} - V_f$$

TD where is the apparent density of the carbon in $g.cm^{-3}$; W is the weight of the carbon weighed in g; V is the actual volume occupied by the weight of activated carbon in cm^3; Vep is the volume of the test tube and V is the total volume occupied by the carbon and the fluid.

Determination of pore volume: The porous volume is calculated from the apparent density and the actual density using the following formula:

$$V_P = \frac{1}{BD - TD}$$

$V_P$where V is the porous volume; BD is the bulk density in $g.cm^{-3}$; TD is the true density in $g.cm^{-3}$.

Determination of porosity: Porosity is one of the essential parameters that characterize adsorbents. It represents the fraction of the void space in activated carbon relative to its total volume, including the inter-particle void space (Waji, 2018). It is determined by using the following formula:

$$\varepsilon = \frac{V_P}{V_T} \times 100$$

ε where is the porosity of the material in %; V_P is the void volume in cm^3; V_T is the total volume of the empty test piece incm^3.

Determination of iodine index: The iodine index is determined according to AWWA B 600 – 78(Maazou et al., 2017). A known mass of the adsorbent, previously dried at 105°C for 24 hours, is placed in contact with a solution of iodine of known volume and concentration and stirred. After filtration, a known volume of the filtrate is titrated with sodium thiosulphate in the presence of starch. The iodine index is determined using the following formula:

$$I_I = \frac{(C_i - C_f) \times V}{m_{CA}}$$

I_I being the iodine index in $mg.g^{-1}$; C_i, the initial weight concentration of iodine in $mg.L^{-1}$; C_f, the final weight concentration of iodine in $mg.L^{-1}$; V, the volume of the adsorbed iodine solution in L; and w_{AC}, the weight of adsorbent in g.

Determination of methylene blue index: The methylene blue index is determined by using the method described in the work of DAS (Das, 2014). A known mass of pre-dried adsorbent is placed in contact with a solution of known concentration of methylene blue for 30 minutes under continuous stirring. The suspension is then filtered, and the residual concentration of methylene blue is determined using a UV spectrophotometer (Agilent Technologies Cary 60 UV-Vis) at a wavelength (λ) of 654 nm. The methylene blue index is determined by the following formula:

$$I_{BM} = \frac{(C_i - C_f) \times V}{m_{CA}}$$

$I_{BM}$is the methylene blue index in $mg.g^{-1}$, C_i the initial weight concentration of methylene blue in $mg.L^{-1}$, C_f the final weight concentration of methylene blue in $mg.L^{-1}$, V the volume of the adsorbed methylene blue solution in L, w_{AC} the weight of adsorbent in g.

Determination of functional groups: Fourier Transform Infrared Spectroscopy (FTIR) was used to determine the nature of the functional groups on the surface of the adsorbents. A spectrometer (FT-IR PerkinElmer Spectrum Two) coupled with a digital computer capable of plotting spectra between 4000 and 400 cm^{-1} was used.

Scanning electron microscope analysis: The morphological analysis of the activated carbon surface was performed using scanning electron microscopy (SEM) with a Hitachi S800 microscope at different magnifications (X 300, X 1000 and X 2500).

Determination of pH of point zero charge (pH_{PZC}): The pH of point of zero charge (pH_{PZC}) was determined according to the protocol proposed by BOUDRAHEM et al. (Saidi et al., 2019). 50 mL solutions of 0.01 M NaCl were prepared in several Erlenmeyer flasks. Their pH values were adjusted to the desired values using 0.01 M NaOH or HCl solutions. Once the pH was constant, approximately 0.15 g of adsorbent was added to each Erlenmeyer flask. The Erlenmeyer flasks are sealed and shaken for 24 hours. The filtrates are then recovered, and their pH is measured again. The final pH curve as a function of the initial pH is used to determine the pH_{PZC}, corresponding to the intersection point of this curve with the first bisector.

Evaluation of activated carbon performance for the removal of a mixture of dye and heavy metals: The effectiveness of activated carbon for wastewater treatment was assessed by studying its performance in removing a mixture of dye and heavy metals (methylene blue, copper, nickel and iron) in aqueous solution.

Adsorption of complex mixtures: Adsorption tests were carried out in a stirred batch reactor in 250 mL mini reactors at room temperature (approximately 25°C) and at a stirring speed of 400 rpm. The effects of contact time, adsorbent dose, initial pollutant concentration, temperature and pH are studied. After each adsorption test, the solutions are filtered through filter paper and the filtrates are analyzed to determine the residual pollutant concentration. The dye and heavy metal contents are determined by UV-Vis spectroscopy (Agilent Cary 60 spectrophotometer) and Atomic Absorption Spectroscopy (AAS) (Spectro Technologies, Thermo Scientific, iCE 3000 Series), respectively. The adsorption capacity and removal rate are calculated using flowing equations:

$$Q_e = \frac{(C_i - C_f) \times V}{m_{CA}}$$

$$E = \frac{(C_i - C_f)}{C_i} \times 100$$

$Q_e$being the adsorption capacity in $mg.g^{-1}$, C_i is the initial weight concentration of MB in $mg.L^{-1}$, C_f is the weight concentration of the solution after adsorption in $mg.L^{-1}$, V is the volume of the solution in L, and T is the MB removal rate in %.

Optimisation of the adsorption process: The operating parameters for the adsorption of the dye and heavy metal mixture (BM, Ni(II), Cu(II) and Fe(II)) are optimised using the single factor at a time methodology. This approach consists of studying the effect of each factor individually while keeping the other parameters constant. The experimental range selected for the adsorption of the mixture is presented in **Table 1**.

Table 1. Experimental areas of pollutant adsorption studied (Diop et al., 2022; Ndiaye et al., 2022)

Parameters	Range and level	
	Low values	High values
Adsorbent dose ($g.L^{-1}$)	0,5	3
Contact time (min)	15	90
Initial concentration ($mg.L^{-1}$)	25	100
pH	4	10

Modelling of adsorption kinetics and isotherms: To better understand the mechanism of pollutant adsorption in a complex mixture and to determine the equilibrium adsorption capacities and maximum adsorption capacities of coal for each of these pollutants, adsorption kinetics and isotherms were modelled (**Table 2**). The kinetic models chosen were the pseudo-first order, pseudo-second order, intra-particle diffusion and Elovich models (**Table 3**), while for the isotherms, the models studied were the Langmuir and Freundlich models.

RESULTS AND DISCUSSION

Physicochemical parameters of activated carbon: The results presented in Table 2 show that activated carbon contains low moisture (2.21%) and ash (1.13%) content, suggesting its high potential as an adsorbent. The bulk density value (0.53 g.cm-3) falls within the typical range (0.20 to 0.55 $g.cm^{-3}$) for activated carbons used in wastewater treatment(Baghel et al., 2011). This is an advantage for its industrial use as an adsorbent. The high porosity of the charcoal (61.06%), ranging from 40 to 85% according to AWWA, indicates a highly developed structure that is suitable for industrial use in water treatment(Elango & Govindasamy, 2018). The pore volume (1.15 $cm^3.g^{-1}$) of activated carbon is comparable to that of activated carbons based on coconut shells (Nieto-Delgado et al., 2011) and rubber (Yousatit et al., 2020) (1.14 - 1.44 $cm^3.g^{-1}$), chitosan (0.67 - 1.39 $cm^3.g^{-1}$) (Wang et al., 2021), cow dung (1.13 $cm^3.g^{-1}$) (Demiral & Demiral, 2008).This confirms that neem husks are a good precursor to produce commercial activated carbon. The high methylene blue (39.21 $mg.g^{-1}$) and iodine (788.20 $mg.g^{-1}$) indices of the activated carbon reflect the heterogeneity of its porosity.

Table 2. Equations of kinetic models

Models	Equations	Curves	Parameters
Pseudo-premier ordre	$\frac{1}{Q_t} = \frac{K_1}{Q_e}\frac{1}{t} + \frac{1}{Q_e}$	$\frac{1}{Q_t}\ vs\ \frac{1}{Q_e}$	**Q_t:** adsorption capacity at time t in mg.g^{-1} ; **K_1:** pseudo-first-order rate constant in min^{-1}; **t :** contact time in min ; **Q_e:** equilibrium adsorption capacity in mg.g^{-1}.
Pseudo-second ordre	$\frac{t}{Q_t} = \frac{1}{Q_e}t + \frac{1}{K_2 Q_e^2}$	$\frac{t}{Q_t}\ vs\ t$	**Q_t:** quantity of solute adsorbed by the material at time t in mg.g^{-1} ; **K_2:** apparent rate constant of the pseudo-second order in g.mg^{-1}.min^{-1}; **Q_e:** adsorption capacity at equilibrium in mg.g^{-1}.
Diffusion intraparticulaire	$Q_t = K_{int}.t^{1/2} + C$	Q_t vs $t^{1/2}$	**Q_t:** adsorption capacity at time t in mg.g^{-1}; **K_{int}:**rate constant of intra-particle diffusion in mg.g^{-1}.min^{-1}; **C:** the constant related to the thickness of the boundary layer in mg.g^{-1}.
Elovich	$Q_t = \frac{1}{\beta} lnt + \frac{1}{\beta} ln(\alpha\beta)$	$Q_t$vs lnt	**Q_t:** adsorption capacity at time t in g.mg^{-1}; **α:** initial adsorption rate in mg.g^{-1}.min^{-1}; **β:** desorption constant in g.mg^{-1}.

Table 3. Equations of the isotherm models studied

Models	Equations	Curves	Parameters
Freundlich	$lnQ_e = \frac{1}{n} lnC_e + lnK_F$	$lnQ_e\ vs\ lnC_e$	Q_e: equilibrium adsorption capacity in mg.g^{-1}; C_e: equilibrium solute concentration in mg.L^{-1}; K_F and n: empirical constants (dimensionless) to be determined.
Langmuir	$\frac{C_e}{Q_e} = \frac{1}{Q_{max}} C_e + \frac{1}{bQ_{max}}$	$\frac{C_e}{Q_e}\ vs\ C_e$	Q_e:amount of BM adsorbed at equilibrium in mg.g^{-1}; Q_{max}:maximum amount adsorbed at monolayer saturation or maximum adsorption capacity in mg.g^{-1}; C_e: weight concentration at equilibrium in mg.L^{-1}; b: is the Langmuir constant.
Temkin	$Q_E = B_T \ln C_e + B_T \ln A_T$	Q_E vs$\ln C_e$	Q_e:amount of BM adsorbed at equilibrium in mg.g^{-1}; C_e: weight concentration at equilibrium in mg.L^{-1}; R: ideal gas constant in J.K^{-1}.mol^{-1}; T: absolute temperature in K; B_T: constant related to adsorption heat; A_T: constant related to equilibrium in L.mg^{-1}. b: Temkin isotherm constant related to adsorption heat.

Table 4. Physicochemical parameters of activated carbon

Parameters	Units	Values	AWWAstandard(Nicholson, 1887)
Moisture content	%	2.21	5-8
Ash content	%	1.13	5-15
Bulk density	g.cm^{-3}	0.5320	0.25
True density	g.cm^{-3}	1.2028	-
Pore volume	cm^3.g^{-1}	1.1416	-
Porosity	%	61.06	40 – 85
Methylene blue indexmethylene	mg.g^{-1}	39.21	> 450
Iodine index	mg.g^{-1}	788.20	600 -1100
pH	-	4.48	6 – 8
pH_{PZC}	-	6.05	-
Electric conductivity électrique	µs.m^{-1}	252.40	-

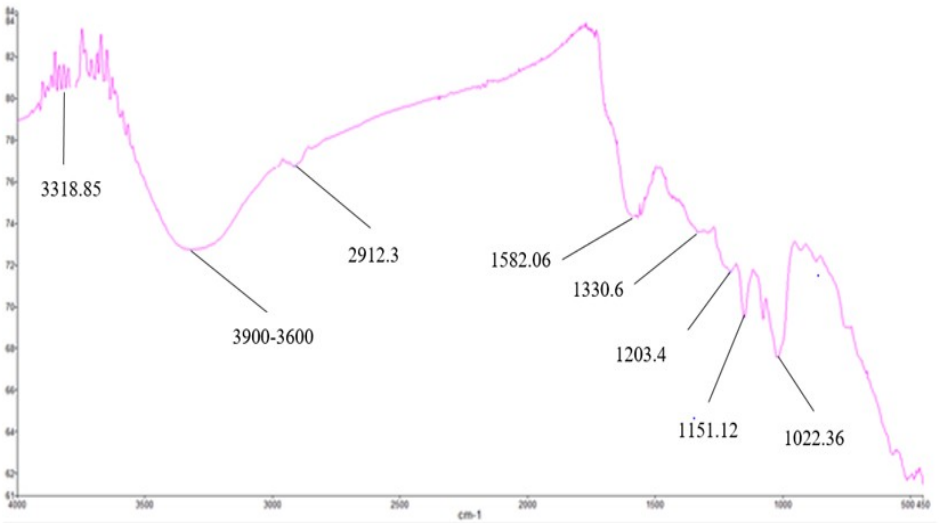

Fig. 4. Fourier Transform Infrared Spectrum of Activated Carbon

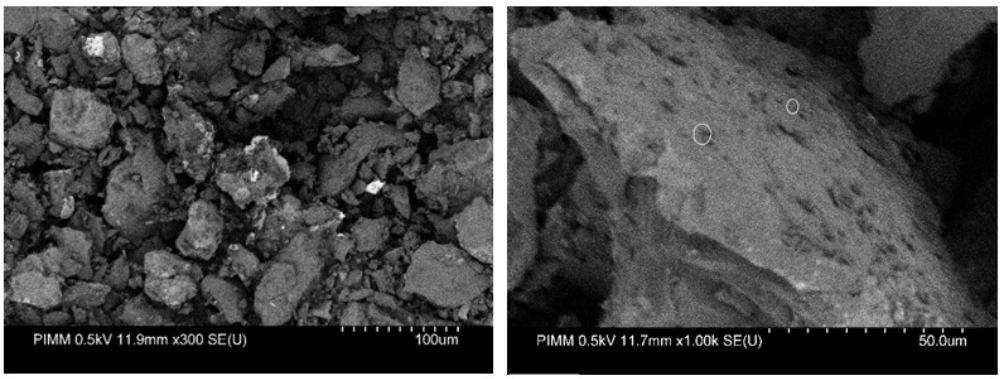

(a) (b)

Fig. 5. SEM images of activated carbon (magnification ×300 (a), ×1000 (b))

Table 5. Kinetic parameters of the adsorption of the mixture on activated carbon based on neem shells

Parameters	Cu(II)	Ni(II)	Fe(II)	BM
Pseudo-first order model				
Q_e	7.59	24.69	16.84	25.12
K_1	43.83	0.156	2.33	0.28
R^2	98.22	72.42	98.13	95.90
Pseudo-second order model				
Q_{max}	6.58	24.75	16.78	25.06
K_2	0.11	$1.88.10^{-5}$	0.0004	$1,29.10^{-5}$
R^2	97.34	100	99.99	100
Diffusion intraparticulaire model				
K_p	0.50	0.04	0.30	0.06
C	0.35	24.28	13;75	24.50
R^2	90.08	90.81	82.39	70.30
Elovich model				
A	0.39	1.37E+79	192944,48	2.77E+52
B	0.62	7.65	1.01	5.06
R^2	95.75	86.18	90.48	81.26

Table 6. Parameters of the isotherms studied

Polluants	BM	Cu(II)	Ni(II)	Fe(II)
Langmuir model				
Q_{max}	52.08	6.17	66.67	25.12
B	48.00	0.22	0.34	0.17
R^2	99.44	99.02	95.30	97.08
Freundlich model				
K_F	61.31	3.28	16.73	9.71
N	4.30	7.70	1.76	4.77
R^2	98.98	96.38	99.28	95.93
1/n	0.23	0.13	0.57	0.21
Temkin model				
B_T	0,62	7,65	1,01	5,06
A_T	0,39	$1,37.10^{79}$	$1,93.10^{5}$	$2,77.10^{52}$
R^2	95,75	86,18	90,48	81,26

The iodine index value confirms that the activated carbon produced complies with AWWA standards (600–1100 $mg.g^{-1}$) for wastewater treatment (Adib et al., 2016; Wagner & Jula, 2018; Yusufu et al., 2012). The pH_{PCN} of the activated carbon is 6.05 (Table 4). This means that when the pH in the solution is below 6.05, the surface charge of the activated carbon is positive, thus promoting the adsorption of anions for this pH range. On the other hand, at pH values above 6.05, the surface of the activated carbon becomes negatively charged, promoting the adsorption of cations (Begum et al., 2021; Kalidou & El Hadji Moussa, 2022). Finally, its electrical conductivity (252.4 $\mu S.cm^{-3}$) is close to those reported in the literature (Elango & Govindasamy, 2018).

Structural analysis of activated carbon

Structural analysis of activated carbon by Fourier Transform Infrared Spectroscopy (FTIR): The FTIR spectrum of activated carbon (Figure 4) shows a broad band between 3000 and 3600 cm^{-1} with a maximum at 3318.85 cm^{-1}, which can be attributed to the presence of a hydroxide (OH) group from alcohol, phenol, and carboxylic acid function(Jawad et al., 2021; Vyavahare et al., 2018). The low-intensity bands between 3600 and 3900 cm^{-1}indicate the presence of free OH groups from water adsorbed by the activated carbon (Kaçan & Kütahyalı, 2012). The presence of a band at 2912.3 cm^{-1}characteristic of an aliphatic C-H bond in alkanes was also noted (Abou Oualid et al., 2020). An intense band with a peak at 1582.06 cm^{-1}could be attributed to the stretching vibration of the carboxyl group C=O of carboxylic, ketone, aldehyde, lactone, or ester functions or to the C=C stretching of aromatic groups(Jawad et al., 2021; Sahu et al., 2010).The peaks at 1151.12cm-1 and 1022.36 $cm^{-1}$are attributed to vibrations of C-O bonds in alcohols, ether oxides, Esters (Akhouairi et al., 2019; Fernandez et al., 2014; Jawad et al., 2021; Li et al., 2015; Pan et al., 2016), or carboxylic groups to vibrations of phosphoric groups (P-O) in esters (P-O-C or P-O-P) or (P=O) (Pan et al., 2016). The presence of phosphoric groups (P-O, P=O and P-O-P) on the surface of activated carbon may result from the impregnation process. The low-intensity bands at 1203.4 cm-1 and 1330.6 cm^{-1}may

be due to vibrations of the $–CH_2$ and $-CH_3$ bonds(Abou Oualid et al., 2020; Jawad et al., 2021; Vyavahare et al., 2018).

Overall, the FTIR spectrum of activated carbon shows that the functional groups present on the surface of activated carbon are alcohols, carboxylic acids, esters, aldehydes, ketones, ether oxides and lactones. The presence of these multiple and diverse functional groups can make the surface of the carbon more reactive.

Morphological analysis of activated carbon by SEM: Low magnification scanning electron microscopy images (**Figure 5a**) show irregular particle size and shape in the carbon powder. Those at higher magnifications (**Figures 5b**) also show a highly porous morphology of the activated carbon, with the presence of several cavities of different sizes and shapes, corroborating the development of heteroporousness on the surface of the carbon. The heterogeneous development of the carbon's porosity suggests a high capacity for binding various molecules (dyes, heavy metals, pesticides, fats, etc.)(Pehlivan, 2018; Wang et al., 2020)

Optimisation of operating parameters for mixture removal

Influence of contact time on mixture adsorption: The evolution of the quantity of adsorbed pollutants shows two distinct phases for all pollutants. The first corresponds to rapid adsorption characterised by a significant increase in the quantity retained, followed by a phase in which the variation becomes small until equilibrium is reached, reflecting the gradual saturation of the activated carbon. This initially rapid absorption is also facilitated by a high driving force, which then decreases under the effect of electrostatic repulsion (Wang et al., 2023). The equilibrium time depends on the nature of the pollutant: it is reached in 15 minutes for BM and Ni(II) ions, compared to 60 and 75 minutes for Cu(II) and Fe(II), respectively. This difference can be explained by the complexity of the mechanisms involved, such as ion exchange, precipitation, complexation, electrostatic attraction, or physical adsorption (Ifthikar et al., 2018).

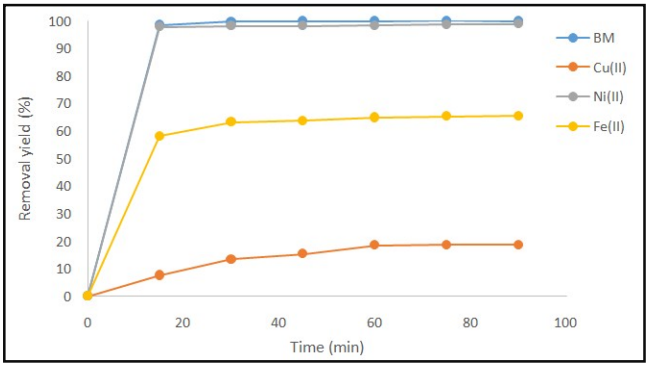

Fig. 6. Kinetics of mixture removal on activated carbon ***(C_0 = 50 mg.L^{-1}; m = 0,1 g; V = 100 mL; T = 25°C)***

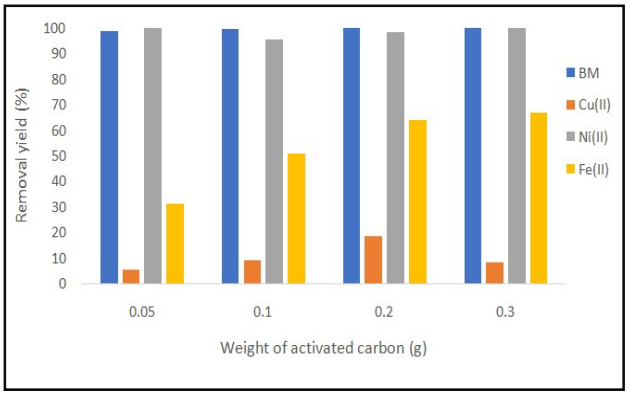

Fig. 7. Effect of adsorbent weight on mixture removal ***(C_0 = 50 mg.L^{-1}; t = 120 min; V =100 mL; T = 25°C)***

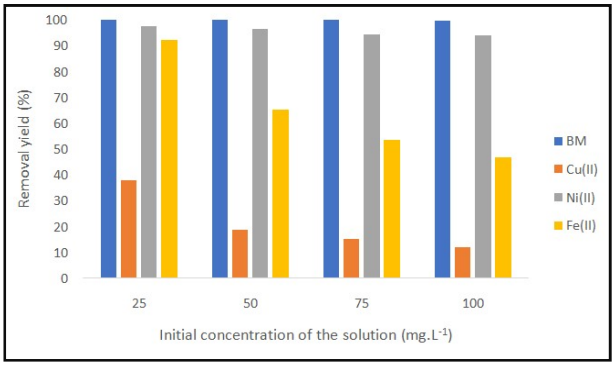

Fig. 8.Effect of initial concentration on mixture removal ***(T = 60 min; m = 0,1 g; V = 100 mL; T = 25°C)***

Influence of adsorbent mass on mixture adsorption: The amount of pollutant adsorbed generally increases forth with the mass of adsorbent, particularly for Cu (II) and Fe(II) ions, while the removal of BM and Ni(II) ions varies just a little. Thus, when the mass of adsorbent increases from 0.05 to 0.2 g, the removal rate of Fe(II) ions increases from 31.18 to 63.74%, while that of Cu(II) ions decreases from 50.50 to 18.52%. This trend can be explained by the increase in the exchange surface area and the number of adsorption sites (Diop et al., 2022; Tsamo et al., 2019). On the other hand, BM and Ni(II) ions are almost completely removed at the lowest mass. Above 0.2 g, removal increases slightly for all pollutants.

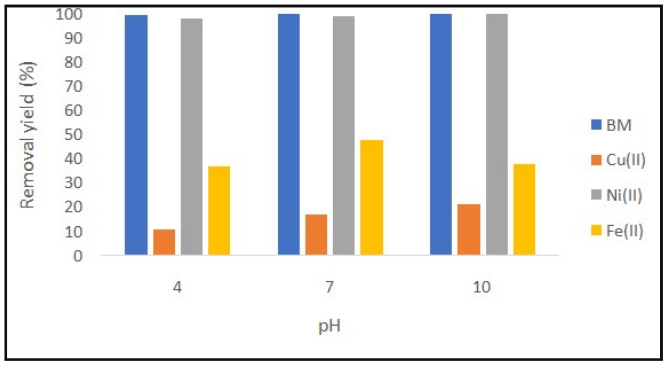

Fig. 9. Effect of the pH of the initial solution on the removal of the mixture ***(C_0 = 50 mg.L^{-1}; m=0.1 g; t = 120 min; V=100 mL; T = 25°C)***

Influence of initial pollutant concentration on mixture adsorption: The elimination rate is strongly influenced by the nature of the pollutant and tends to decrease with increasing initial concentration of the solution, regardless of the species studied. The established order of affinity (BM > Ni(II) > Fe(II) > Cu(II)) remains constant regardless of the initial concentration of the pollutant. This affinity hierarchy can be explained by the intrinsic physicochemical properties of the different species, in particular the ionic radius, hydrated radius, electronegativity, and hydrolysis constant of the metal ions. Indeed, the order of ionic and hydrated radii follows the order Fe(II) > Cu(II) > Ni(II), while electronegativities follow the sequence: Ni(II) (1.91) > Cu(II) (1.90) > Fe(II) (1.85). The strong affinity of charcoal for Ni(II) ions can be explained by its low ionic and hydrated radii, which promotes better diffusion through the pores of the adsorbent and increased fixation (Imaga et al., 2015). The affinity of carbon for Fe(II) ions may be linked to the developed macroporosity of carbon, as evidenced by the methylene blue index. This trend may also be due to the difference in electronegativity between the species (Abdi et al., 2018). This difference in affinity may also be due to the types of bonds formed between the adsorbed pollutants and the surface functional groups of the adsorbent (phenol, hydroxyl, carboxyl, carbonyl, semi-quinone, sulfonate, amine, amide groups, etc.) (Ifthikar et al., 2018; Ramirez et al., 2020; Supong et al., 2020). Cu(II) ions generally bind with carboxyl groups, forming ring-shaped complexes with multi-dentate chelating compounds, whereas Ni(II) and Fe(II) ions have 1:1 stoichiometric relationships (Mahdi et al., 2019).

Influence of pH on mixture adsorption: The variation in the removal rate as a function of pH depends on the nature of the pollutant, while maintaining the same order of affinity regardless of pH. This rate changes little with pH for BM and Ni(II) ions, but increases rapidly with Cu(II) ions. On the other hand, it decreases above pH 7 with Fe(II) ions, probably due to their precipitation. The optimal pH for removal is 10 for all the pollutants studied, with the exception of Fe(II) ions, for which the optimum is reached at pH 7. The increase in dye and Cu(II) metal ion fixation at pH values above pH_{PZC} (6.05) can be explained by the negative charge on the surface of the activated carbon, which promotes electrostatic attraction with metal cations at pH values below the pH_{PZC} of the carbon. the surface of the carbon is positively charged, leading to increased competition between H^+ ions and pollutants, as well as electrostatic repulsion that is unfavorable to their adsorption(Campos et al., 2020).

Modelling the adsorption kinetics of the mixture: The modelling results (**Table 5**) show that the pseudo-second-order model is the most suitable model for describing the binding of pollutants to the activated carbon surface, with correlation coefficients of 97.34, 100, 99.99 and 100 for Cu(II), Ni(II), Fe(II) and BM ions, respectively. The high values indicate that the mechanism is chemisorption(Sherugar et al., 2022). The low coefficients of determination obtained with the intra-particle diffusion model for all pollutants also indicate that this mechanism is not a decisive step in the adsorption process of the multi-component system. The equilibrium adsorption capacities calculated using the pseudo-second order model are 25.06, 6.58, 24.75 and 16.78 $mg \cdot g^{-1}$ for BM, Ni(II), Cu(II) and Fe(II), respectively. These results confirm that carbon is more effective at removing dye than metal ions. However, it is more effective at removing Ni(II) ions than other metal ions. The adsorption rates (K_2) show that the binding of the ions studied on the surface of the activated carbon depends on the nature of the pollutant. The order of binding rate is as follows: BM > Ni(II) > Fe(II) > Cu(II). The difference in binding rate may be due to the difference in the types of bonds between the adsorbed species and the functional groups of the activated carbon (Kim & Kim, 2020).

Modelling of adsorption isotherms for the mixture: The Langmuir model best describes the adsorption of BM, Cu(II) and Fe(II) ions, indicating single-layer sorption chemistry on a homogeneous surface, while the adsorption of Ni(II) ions is explained by the Freundlich model, reflecting multi-layer adsorption on a heterogeneous surface (El Maguana et al., 2020) (**Table 6**). The relatively high correlation coefficients obtained with the Freundlich model for BM, Cu(II) and Fe(II) show that their adsorption can also be described by this model. On the other hand, the low correlation coefficients associated with the Temkin model indicate that the biosorption of these species is not correctly represented by this model. This difference in binding mechanism may be due to differences in the physicochemical properties of the species studied(Kouakou et al., 2013; Tran et al., 2020).The maximum adsorption capacities predicted by the Langmuir model are 52.08 $mg.g^{-1}$ (BM), 6.17 $mg.g^{-1}$(Cu(II)), 66.67 $mg.g^{-1}$(Ni(II)) and 25.12 $mg.g^{-1}$(Fe(II)). These results show that activated carbon is more effective for dyes than for metal ions, with selectivity varying depending on the ions (Agbozu & Emoruwa, 2014; Alslaibi et al., 2014; Imaga et al., 2015). In the literature, the maximum adsorption capacities for binding the pollutants studied are higher than those for the adsorption of Cu(II), Cd(II) and Ni(II) on fly ash in a multi-component system (BM, Cu(II), Ni(II) and Fe(II))(Visa et al., 2010), but remain low compared to other activated carbons.

The affinity of the adsorbent depends on the nature of the pollutant to be adsorbed and the nature of the adsorbent. The order of selectivity is as follows: Ni(II) > Cu(II) > Fe(II) for activated carbon based on olive pit waste (Alslaibi et al., 2014), while for adsorbents based on raw and activated sorghum husks, according to IMAGA et al. (2015), it is: Ni(II) > Cu(II) (Imaga et al., 2015). However, it is Fe(II) > Cu(II) for activated carbon based on coconut shells, according to the work of AGBOZU (Agbozu & Emoruwa, 2014). The K_F and n constants of Freundlich are indicators of adsorption capacity and intensity, respectively (Aksu, 1998; El Maguana et al., 2020). The higher the values of these K_F and n constants, the easier it is for the adsorbate to bind to the surface of the adsorbent(Kassa et al., 2019; Kim & Kim, 2020). The values of these constants for BM and Ni(II) and Fe(II) ions indicate a strong affinity of activated carbon for these molecules(Agbozu & Emoruwa, 2014). The values of the heterogeneity factors (1/n), which are less than 1, confirm the affinity of activated carbon for these molecules and confirm the nature of chemisorption-type adsorption. This result is consistent with those of the kinetic study.

CONCLUSION

The treatment of wastewater before its discharge into the receiving environment is now a necessity for the preservation of the environment. The objective of this study was to develop activated carbon from neem shells and to evaluate its effectiveness in removing a complex mixture of dyes and heavy metals. Characterisation of the activated carbon showed good adsorption performance, confirmed by high methylene blue and iodine indices. Kinetic analysis showed that adsorption follows the pseudo-second-order model for BM, Cu(II) and Fe(II) ions, while that of Ni(II) ions is better described by the pseudo-first-order model. Modelling of the adsorption isotherms showed that the Langmuir model applies to all pollutants except Ni(II) ions, for which the Freundlich model is more suitable. The results also highlight a difference in the affinity of the pollutants studied. Overall, neem shell-based activated carbon is more effective at removing dyes than heavy metals, with an affinity order for the latter of Ni(II) > Fe(II) > Cu(II). These differences reflect distinct binding mechanisms depending on the adsorbate. In summary, this study demonstrates that neem shells are an excellent precursor to produce activated carbon suitable for wastewater treatment, particularly wastewater containing both dyes and heavy metals. To complement this study, it would be interesting to evaluate the effectiveness of activated carbon in treating real wastewater, as well as in removing other recalcitrant molecules such as pesticides and pharmaceutical compounds.

Key points: Valorisation of neem (*Azadirachta indica* A. Juss) seed shells, co-products of neem seed exploitation, through the production of activated carbon; Evaluation of the performance of activated carbon developed for the removal of a mixture of dyes and heavy metals; Modelling of adsorption kinetics and isotherms.

ACKNOWLEDGEMENTS

We thank all the technical staff of the Chemical Engineering Laboratory of Polytechnique Higher School of Dakar (ESP). We would also like to express our sincere thanks to Dr Mamadou Lamine SENE and M. Mamadou SENE for the time and effort they devoted to proofreading and correcting this article.

Funding: The authors declare that no funds, grants, or other support were received during the preparation of this manuscript.

Author Contributions

Adama DIOP: Methodology, Validation, data curation, Writing-original draft, Writing-review and editing, Visualization Mamadou FAYE: Conceptualization, Writing-original draft, Writing-review and editing, Project administration Djibril DIEDHIOU:Wriiting-review and editingPapa Lat Dior DIOP:Wriiting-review and editingMbaye WADE:data curation, Wriiting-review and editing Wriiting-review and editingCodou Guèye Mar DIOP: Supervision, Writing-review and editing.

Ethical Approval: Thisarticle does not contain any studies involving human or animal subjects.

Consent to participat : This article does not contain any studies involving human or animal subjects.The authors attest that there is no consent to participate to declare.

Consent to publish : This article does not contain any studies involving human or animal subjects.The authors attest that there is no consent to publish to declare.

Declaration of Competing Interest: The authors report no declarations of interest.

Data Availability Statement: The authors declare that the data supporting the findings of this study are available within the paper and its Supplementary Information files. Should any raw data files be needed in another format they are available from the corresponding author upon reasonable request.

REFERENCES

Abdi, G., Alizadeh, A., Zinadini, S., & Moradi, G. (2018). Removal of dye and heavy metal ion using a novel synthetic polyethersulfone nanofiltration membrane modified by magnetic graphene oxide/metformin hybrid. *Journal of membrane science*, *552*, 326-335.

Abou Oualid, H., Abdellaoui, Y., Laabd, M., El Ouardi, M., Brahmi, Y., Iazza, M., & Abou Oualid, J. (2020). Eco-efficient green seaweed codium decorticatum biosorbent for textile dyes: characterization, mechanism, recyclability, and RSM optimization. *ACS omega*, *5*(35), 22192-22207.

Adib, M., Suraya, W., Rafidah, H., Amirza, A., Attahirah, M., Hani, M., & Adnan, M. (2016). Effect of phosphoric acid concentration on the characteristics of sugarcane bagasse activated carbon. IOP conference series: materials science and engineering,

Agbozu, I., & Emoruwa, F. (2014). Batch adsorption of heavy metals (Cu, Pb, Fe, Cr and Cd) from aqueous solutions using coconut husk. *African Journal of Environmental Science and Technology*, *8*(4), 239-246.

Ahsaine, H. A., Anfar, Z., Zbair, M., Ezahri, M., & El Alem, N. (2018). Adsorptive removal of methylene blue and crystal violet onto micro-mesoporous Zr3O/activated carbon composite: a joint experimental and statistical modeling considerations. *Journal of Chemistry*, *2018*, 1-14.

Akhouairi, S., Ouachtak, H., Addi, A. A., Jada, A., & Douch, J. (2019). Natural sawdust as adsorbent for the eriochrome black T dye removal from aqueous solution. *Water, Air, & Soil Pollution*, *230*(8), 181.

Aksu, Z. (1998). Biosorption of heavy metals by microalgae in batch and continuous systems. *Wastewater treatment with algae*, 37-53.

Alslaibi, T. M., Abustan, I., Ahmad, M. A., & Abu Foul, A. (2014). Preparation of activated carbon from olive stone waste: optimization study on the removal of Cu2+, Cd2+, Ni2+, Pb2+, Fe2+, and Zn2+ from aqueous solution using response surface methodology. *Journal of dispersion science and technology*, *35*(7), 913-925.

Anfar, Z., Ait Ahsaine, H., Zbair, M., Amedlous, A., Ait El Fakir, A., Jada, A., & El Alem, N. (2020). Recent trends on numerical investigations of response surface methodology for pollutants adsorption onto activated carbon materials: A review. *Critical Reviews in Environmental Science and Technology*, *50*(10), 1043-1084.

Ani, J., Akpomie, K., Okoro, U., Aneke, L., Onukwuli, O., & Ujam, O. (2020). Potentials of activated carbon produced from biomass materials for sequestration of dyes, heavy metals, and crude oil components from aqueous environment. *Applied Water Science*, *10*(2), 1-11.

Baghel, A., Singh, B., Prasad, G., Pandey, P., & Gutch, P. (2011). Preparation and characterization of active carbon spheres prepared by chemical activation. *Carbon*, *49*(14), 4739-4744.

Begum, B., Ijaz, S., Khattak, R., Qazi, R. A., Khan, M. S., & Mahmoud, K. H. (2021). Preparation and characterization of a novel activated carbon@ polyindole composite for the effective removal of ionic dye from water. *Polymers*, *14*(1), 3.

Campos, N. F., Guedes, G. A., Oliveira, L. P., Gama, B. M., Sales, D. C., Rodriguez-Diaz, J. M., Barbosa, C. M., & Duarte, M. M. (2020). Competitive adsorption between Cu2+ and Ni2+ on corn cob activated carbon and the difference of thermal effects on mono and bicomponent systems. *Journal of environmental chemical engineering*, *8*(5), 104232.

Das, S. (2014). *Characterization of activated carbon of coconut shell, rice husk and Karanja oil cake*

Demiral, H., & Demiral, İ. (2008). Surface properties of activated carbon prepared from wastes. *Surface and Interface Analysis: An International Journal devoted to the development and application of techniques for the analysis of surfaces, interfaces and thin films*, *40*(3-4), 612-615.

Diop, A., Faye, M., Diedhiou, D., Diop, P. L. D., & Diop, C. M. (2022). Valorization of neem, Azadirachta indica A. Juss, seeds hulls as bioadsorbant: Application to the removal of a dye (methylene blue). *Afrique SCIENCE*, *20*(6), 100-120.

Donkadokula, N. Y., Kola, A. K., Naz, I., & Saroj, D. (2020). A review on advanced physico-chemical and biological textile dye wastewater treatment techniques. *Reviews in environmental science and bio/technology*, *19*(3), 543-560.

El Maguana, Y., Elhadiri, N., Benchanaa, M., & Chikri, R. (2020). Activated carbon for dyes removal: modeling and understanding the adsorption process. *Journal of Chemistry*, *2020*, 1-9.

Elango, G., & Govindasamy, R. (2018). Analysis and utilization of temple waste flowers in Coimbatore District. *Environmental Science and Pollution Research*, *25*(11), 10688-10700.

Fernandez, M. E., Nunell, G. V., Bonelli, P. R., & Cukierman, A. L. (2014). Activated carbon developed from orange peels: Batch and dynamic competitive adsorption of basic dyes. *Industrial crops and products*, *62*, 437-445.

Ifthikar, J., Jiao, X., Ngambia, A., Wang, T., Khan, A., Jawad, A., Xue, Q., Liu, L., & Chen, Z. (2018). Facile one-pot synthesis of sustainable carboxymethyl chitosan–sewage sludge biochar for effective heavy metal chelation and regeneration. *Bioresource technology*, *262*, 22-31.

Imaga, C., Abia, A., & Igwe, J. (2015). Adsorption isotherm studies of Ni (II), Cu (II) and Zn (II) ions on unmodified and mercapto-acetic acid (MAA) modified sorghum hulls. *International Research Journal of Pure and Applied Chemistry*, *5*(4), 318.

Jawad, A. H., Abdulhameed, A. S., Wilson, L. D., Syed-Hassan, S. S. A., ALOthman, Z. A., & Khan, M. R. (2021). High surface area and mesoporous activated carbon from KOH-activated dragon fruit peels for methylene blue dye adsorption: optimization and mechanism study. *Chinese Journal of Chemical Engineering*, *32*, 281-290.

Kaçan, E., & Kütahyalı, C. (2012). Adsorption of strontium from aqueous solution using activated carbon produced from textile sewage sludges. *Journal of Analytical and Applied Pyrolysis*, *97*, 149-157.

Kalidou, B., & El Hadji Moussa, D. (2022). Optimization of cristal violet adsorption by calcium silicate waste material. *Scientific African*, *18*, e01417.

Kassa, M., Haile, W., & Kebede, F. (2019). Evaluation of adsorption isotherm models for potassium adsorption under different soil types in Wolaita of Southern Ethiopia. *Communications in soil science and plant analysis*, *50*(4), 388-401.

Kim, M.-S., & Kim, J.-G. (2020). Adsorption characteristics of spent coffee grounds as an alternative adsorbent for cadmium in solution. *Environments*, *7*(4), 24.

Kouakou, U., Yapo, J. A., & Trokourey, A. (2013). Adsorption of iron and zinc on commercial activated carbon. *Journal of environmental chemistry and ecotoxicology*, *5*(6), 168-171.

Ks, G., & Belagali, S. (2013). Removal of heavy metals and dyes using low cost adsorbents from aqueous medium-, a review. *IOSR journal of Environmental Science, toxicology and food technology*, *4*(3), 56-68.

Lakherwal, D. (2014). Adsorption of heavy metals: a review. *International journal of environmental research and development*, *4*(1), 41-48.

Li, Y., Zhang, X., Yang, R., Li, G., & Hu, C. (2015). The role of H 3 PO 4 in the preparation of activated carbon from NaOH-treated rice husk residue. *RSC advances*, *5*(41), 32626-32636.

Maazou, S. D., Hima, H. I., Alma, M. M. M., Adamou, Z., & Natatou, I. (2017). Removal of chromium using activated carbon

developed and characterised from the shell of the Balanites aegyptiaca nut. *International Journal of Biological and Chemical Sciences*, *11*(6), 3050-3065.

Mahdi, Z., Yu, Q. J., & El Hanandeh, A. (2019). Competitive adsorption of heavy metal ions (Pb2+, Cu2+, and Ni2+) onto date seed biochar: batch and fixed bed experiments. *Separation Science and Technology*, *54*(6), 888-901.

Ndiaye, E. M., Ba, K., Sow, A., Diop, A., El Idrissi, Y., El Moudden, H., Faye, P. G., Harhar, H., Ayessou, N., & Tabyaoui, M. (2022). Valorization of natural residue into activated carbon: example of the shells of the African baobab fruit (Adansonia digitata) L. *Journal of Materials Science and Engineering A*, *12*(4-6), 41-54.

Nicholson, F. A. (1887). *Manual of the Coimbatore District in the Presidency of Madras*. Government Press.

Nieto-Delgado, C., Terrones, M., & Rangel-Mendez, J. (2011). Development of highly microporous activated carbon from the alcoholic beverage industry organic by-products. *Biomass and bioenergy*, *35*(1), 103-112.

Ouyang, J., Zhou, L., Liu, Z., Heng, J. Y., & Chen, W. (2020). Biomass-derived activated carbons for the removal of pharmaceutical mircopollutants from wastewater: A review. *Separation and Purification Technology*, *253*, 117536.

Pan, H., Zhao, J., Lin, Q., Cao, J., Liu, F., & Zheng, B. (2016). Preparation and characterization of activated carbons from bamboo sawdust and its application for CH4 selectivity adsorption from a CH4/N2 system. *Energy & Fuels*, *30*(12), 10730-10738.

Pehlivan, E. (2018). Production and characterization of activated carbon from pomegranate pulp by phosphoric acid. *Journal of the Turkish Chemical Society Section A: Chemistry*, *5*(1), 1-8.

Ramirez, A., Ocampo, R., Giraldo, S., Padilla, E., Flórez, E., & Acelas, N. (2020). Removal of Cr (VI) from an aqueous solution using an activated carbon obtained from teakwood sawdust: Kinetics, equilibrium, and density functional theory calculations. *Journal of environmental chemical engineering*, *8*(2), 103702.

Sahu, J., Acharya, J., & Meikap, B. (2010). Optimization of production conditions for activated carbons from Tamarind wood by zinc chloride using response surface methodology. *Bioresource technology*, *101*(6), 1974-1982.

Saidi, S., Boudrahem, F., Yahiaoui, I., & Aissani-Benissad, F. (2019). Agar-agar impregnated on porous activated carbon as a new adsorbent for Pb (II) removal. *Water Science and Technology*, *79*(7), 1316-1326.

Sherugar, P., Padaki, M., Naik, N. S., George, S. D., & Murthy, D. H. (2022). Biomass-derived versatile activated carbon removes both heavy metals and dye molecules from wastewater with near-unity efficiency: Mechanism and kinetics. *Chemosphere*, *287*, 132085.

Supong, A., Bhomick, P. C., Karmaker, R., Ezung, S. L., Jamir, L., Sinha, U. B., & Sinha, D. (2020). Experimental and theoretical insight into the adsorption of phenol and 2, 4-dinitrophenol onto Tithonia diversifolia activated carbon. *Applied Surface Science*, *529*, 147046.

Tran, A. T., Pham, T. T., Nguyen, Q. H., Hoang, N. T., Bui, D. T., Nguyen, M. T., Nguyen, M. K., & Van der Bruggen, B. (2020). From waste disposal to valuable material: Sulfonating polystyrene waste for heavy metal removal. *Journal of environmental chemical engineering*, *8*(5), 104302.

Tsamo, C., Paltahe, A., Fotio, D., Vincent, T. A., & Sales, W. F. (2019). One-, Two-, and Three-Parameter Isotherms, Kinetics, and Thermodynamic Evaluation of Co (II) Removal from Aqueous Solution Using Dead Neem Leaves. *International Journal of Chemical Engineering*, *2019*(1), 6452672.

Visa, M., Bogatu, C., & Duta, A. (2010). Simultaneous adsorption of dyes and heavy metals from multicomponent solutions using fly ash. *Applied Surface Science*, *256*(17), 5486-5491.

Vyavahare, G. D., Gurav, R. G., Jadhav, P. P., Patil, R. R., Aware, C. B., & Jadhav, J. P. (2018). Response surface methodology optimization for sorption of malachite green dye on sugarcane bagasse biochar and evaluating the residual dye for phyto and cytogenotoxicity. *Chemosphere*, *194*, 306-315.

Wagner, N., & Jula, R. (2018). Activated carbon adsorption. In *Activated carbon adsorption for wastewater treatment* (pp. 41-60). CRC Press.

Waji, Y. A. (2018). Bamboo based activated carbon for removal of lead from aqueous solution. *Unpublished Master Thesis, Addis Ababa Science and Technology University, Ethiopia*.

Wang, C., Liu, X., Yang, T., Sridhar, D., Algadi, H., Xu, B. B., El-Bahy, Z. M., Li, H., Ma, Y., & Li, T. (2023). An overview of metal-organic frameworks and their magnetic composites for the removal of pollutants. *Separation and Purification Technology*, *320*, 124144.

Wang, J., Chen, S., Xu, J.-y., Liu, L.-c., Zhou, J.-c., & Cai, J.-j. (2021). High-surface-area porous carbons produced by the mild KOH activation of a chitosan hydrochar and their CO2 capture. *New Carbon Materials*, *36*(6), 1081-1090.

Wang, Y., Wang, S.-l., Xie, T., & Cao, J. (2020). Activated carbon derived from waste tangerine seed for the high-performance adsorption of carbamate pesticides from water and plant. *Bioresource technology*, *316*, 123929.

Yousatit, S., Pitayachinchot, H., Wijitrat, A., Chaowamalee, S., Nuntang, S., Soontaranon, S., Rugmai, S., Yokoi, T., & Ngamcharussrivichai, C. (2020). Natural rubber as a renewable carbon source for mesoporous carbon/silica nanocomposites. *Scientific reports*, *10*(1), 12977.

Yusufu, M., Ariahu, C., & Igbabul, B. (2012). Production and characterization of activated carbon from selected local raw materials. *African journal of pure and applied chemistry*, *6*(9), 123-131.

****